# Failure Analysis Results for Evaluating the Long-Term Reliability of Test Vehicles Assembled with Lead-free Materials


**Authors:**

Greg Morose, Toxics Use Reduction Institute (TURI), Lowell, MA
Sammy Shina, University of Massachusetts, Lowell, MA
Richard Anderson, Cobham, Lowell, MA
Helena Pasquito, EPTAC, Manchester, NH
Paul Bodmer and Bob Farrell, Benchmark Electronics, Hudson, NH
Don Longworth, Dynamics Details Incorporated, Newburyport, MA
Ken Degan, Teradyne Inc., North Reading, MA
Donald Abbott, Texas Instruments, Attleboro, MA
David Pinsky, Karen Ebner, and Amit Sarkhel, Raytheon Company, Tewksbury, MA
Mike Miller, Textron Systems, Wilmington, MA
Charlie Bickford, Wall Industries, Exeter, NH
Deb Fragoza and Eric Ren, EMC, Hopkinton, MA
Don Lockard, Yankee Soldering, East Greenwich, RI
Scott Miller, FreedomCAD, Nashua, NH
Paul Reid and Bill Birch, PWB Interconnect Solutions, Nepean, Ontario
Roger Benson, Carsem, Attleboro, MA
George Wilkish, Prime Consulting


## Abstract


The New England Lead-free Electronics Consortium is a collaborative effort of New England companies spanning the electronics supply chain, sponsored by the Toxics Use Reduction Institute, the U.S. EPA, and the University of Massachusetts Lowell. The consortium has previously completed and published the results from several phases of manufacturing and testing of lead-free Printed Wiring Boards (PWBs) with the goal of achieving lead-free soldering processes with comparable performance and reliability to that of leaded solder processes.

The objective of the current phase of testing (Phase IV) is to address the outstanding rework and long-term reliability issues for lead-free electronics, as well as to evaluate halogen-free laminate materials. The Phase IV test vehicle is comprised of twenty layers, is 0.110” thick, and is densely populated with 900 components on each test vehicle. The research includes the evaluation of ENIG, OSP, HASL, and nano surface finishes, as well as SAC and Sn100C solders. Thirty-six test vehicles were built and inspected to IPC 610 D standards by Benchmark Electronics during 2008. The test vehicles then went through vibration testing at Raytheon test facilities, IST testing at PWB Interconnect Solutions, thermal cycling at Textron Systems and Cobham facilities, and failure analysis at the University of Massachusetts Lowell. In this paper, the authors will present the statistical analysis and overall results of the Phase IV failure analysis.

**Keywords:** Supply chain; lead-free electronics; toxics use reduction; industry collaboration; Design of Experiments

## 1.0 Introduction

Reliability in the electronics industry can be defined as “the ability to function as expected under the expected operating conditions for an expected time period without exceeding expected failure levels”. (Engelmaier, 2008) The reliability of electronics products is a key success factor for many applications in the electronics industry, such as aerospace, medical devices, information technology infrastructure, telecommunications, and defense. The overall reliability of electronic assemblies is a function of many factors including the integrity of the design process, manufacturing process, components, solder joints, cables, connectors, printed circuit board materials, electromagnetic compatibility, and various operating conditions.

The primary focus of this research is the quality of the solder joint. The solder joint can be affected by the transition to lead-free electronics because of the lead-free materials used for the through hole solder, surface mount solder paste, printed circuit board surface finish, and component finish.

Solder joint failures can occur on surface mount components as a result of the differential in thermal expansion between the different assembly materials, vibration during transportation, thermal shock as a result of rapid temperature changes, or mechanical shock from high acceleration events. (IPC, 2002) The objective of the thermal cycling is to induce strain to the solder joints due to the difference in the coefficient of thermal expansions (CTEs) between the different materials in the electronic assembly. There are two major types of thermal expansion that induce strain to the solder joint. The first type is the difference in thermal expansion between the component and the laminate material. The second type is the difference in thermal expansion between the solder and the material to which it is bonded. The formula for calculating this displacement due to differences in thermal expansion is as follows:

$$x = L(\Delta T)(\alpha_A - \alpha_B) \qquad (4)$$

Where x = displacement

L = length of material

$\Delta$ T = Temperature differential

$\alpha_A$ = Coefficient of thermal expansion for material A

$\alpha_B$ = Coefficient of thermal expansion for material B

There are two major categories of surface mount components, leaded and leadless, that have different solder joint reliability characteristics. The surface mount components with leads such as J-leads or gull wing leads, have the ability to absorb the thermal expansion mismatch between the laminate and the component. This occurs because the leads are more compliant than the other parts of the assembly. For leadless surface mount components, such as ball grid arrays, the solder joint absorbs most of the thermal expansion mismatch because the solder is more compliant than the other parts of the structure. (Yasukawa, 1990) Some surface mount components have performance

characteristics of both the leaded and leadless components. For example, thin small outline package (TSOP) components have a high chip to package dimension ratio that can generate large global CTE mismatch between the component and the laminate material. Also, TSOP components have short stiff leads that transfer most of the global CTE mismatch to the solder joint. (MEI, 1996)

## 2.0 Methodology

2.1 Thermal Cycling

Thermal cycle testing to 63% failures was conducted to characterize the failure distribution. This test included continuous resistance monitoring of the daisy chains on the test vehicle by a data logger. Failure is defined as a maximum of 20% nominal resistance increase for a daisy chain circuit within a maximum of five consecutive reading scans.

The Phase IV test vehicle was 8" x 10" in size, had 20 layers, and had a thickness of 0.110 inches. Each of the test vehicles had fourteen daisy chains to monitor solder joint integrity during the actual testing. The intent was to include sixteen test vehicles from the Design of Experiments. These sixteen test vehicles would cover each of the factor combinations in the Design of Experiments. In addition, two test vehicles using the halogen-free laminate would also be included, resulting in a total of eighteen test vehicles for the thermal cycling test. The eighteen test vehicles included in the thermal cycling are listed in the table below.

**Table 1:**
**Test Vehicles Included in Thermal Cycling**

| Test Vehicle | SMT Solder Paste | Through Hole Solder | Surface Finish | PWB Laminate |
|---|---|---|---|---|
| 2 | SAC 305 NC-1 | SAC305 | ENIG | High Tg FR4 |
| 4 | SAC 305 NC-1 | SAC305 | LF HASL | High Tg FR4 |
| 6 | SAC 305 NC-1 | SAC305 | OSP | High Tg FR4 |
| 8 | SAC 305 NC-1 | SAC305 | Nanofinish | High Tg FR4 |
| 10 | SAC 305 OA | Tin/copper (295 C) | ENIG | High Tg FR4 |
| 12 | SAC 305 OA | Tin/copper (295 C) | LF HASL | High Tg FR4 |
| 14 | SAC 305 OA | Tin/copper (295 C) | OSP | High Tg FR4 |
| 16 | SAC 305 OA | Tin/copper (295 C) | Nanofinish | High Tg FR4 |
| 18 | SAC 305 NC-2 | Tin/copper (310 C) | ENIG | High Tg FR4 |
| 20 | SAC 305 NC-2 | Tin/copper (310 C) | LF HASL | High Tg FR4 |

| Test Vehicle | SMT Solder Paste | Through Hole Solder | Surface Finish | PWB Laminate |
|---|---|---|---|---|
| 22 | SAC 305 NC-2 | Tin/copper (310 C) | OSP | High Tg FR4 |
| 24 | SAC 305 NC-2 | Tin/copper (310 C) | Nanofinish | High Tg FR4 |
| 26 | Tin/lead NC | Tin/Lead | ENIG | High Tg FR4 |
| 28 | Tin/lead NC | Tin/Lead | LF HASL | High Tg FR4 |
| 30 | Tin/lead NC | Tin/Lead | OSP | High Tg FR4 |
| 32 | Tin/lead NC | Tin/Lead | Nanofinish | High Tg FR4 |
| 34 | SAC 305 NC-1 | SAC305 | OSP | Halogen free |
| 36 | SAC 305 OA | SAC305 | OSP | Halogen free |

The monitoring during thermal cycling consisted of resistance measurements for the fourteen daisy chain circuits on each of the eighteen test vehicles. The monitoring for the thermal cycling was conducted by using a data logger. The data logger required a total of 252 channels to monitor all of these daisy chains. The data logger equipment used was the Agilent 34980A Multifunction Switch/Measure Unit.

The Agilent data logger is capable of scanning as many as 100 channels per second. Therefore, all 252 channels were able to be scanned in less than five seconds. This scanning rate satisfies the IPC 9701 requirement that the maximum scan interval for all daisy chains be one minute or less.

Four of the fourteen daisy chains on each test vehicle were connected to discrete components (i.e. 0402, 0603, and 0805 resistors). Each of these daisy chains contained approximately 50 - 100 discrete components connected in series. Therefore, monitoring of these daisy chains only detected the first failure for each of the daisy chains on each of the test vehicles. Consequently, we were not able to determine when 63% failure occurs for these discrete components.

The other ten daisy chains on each test vehicle were connected to only one component per daisy chain. The daisy chain is connected to each solder joint of the component. For example, a TSOP component with 48 pins, had all 48 solder joints connected in series. If one solder joint of the component fails, then the data logger detected a failure for that daisy chain. Monitoring of the ten daisy chains with single components provided first failure information for the experiment, as well as when the 63% failure threshold occurred for each component type.

A complete listing of the daisy chain connections is provided in the table below.

**Table 2:**
**Daisy Chain Connections on the Test Vehicle**

| Component RefDes | Component Type | Qty |
|---|---|---|
| R2 to R472 | 0402 Resistor, 0 ohm | 100 |

| Component RefDes | Component Type | Qty |
|---|---|---|
| R21 to R499 | 0603 Resistor, 0 ohm | 100 |
| R5 to R462 | 0805 Resistor, 0 ohm | 49 |
| R15 to R493 | 0805 Resistor, 0 ohm | 52 |
| U1 | SMT, TSOP, 48 Pins | 1 |
| U2 | SMT, TSOP, 48 Pins | 1 |
| U24 | SMT, TSOP, 48 Pins | 1 |
| U25 | SMT, TSOP, 48 Pins | 1 |
| U15 | SMT, PQFP208 | 1 |
| U14 | SMT, Plastic BGA, 256 balls, 1.0 mm pitch | 1 |
| U18 | SMT, Plastic BGA, 256 balls, 1.0 mm pitch | 1 |
| U16 | SMT, Chip array BGA, 100 balls, 1.0 mm pitch | 1 |
| U17 | SMT, Tape array uBGA, 64 balls, 0.5 mm pitch | 1 |
| U26 | SMT, Ceramic u-BGA, 0.5mm pitch | 1 |

The thermal cycling was conducted at the following two locations: the Cobham (M/A-COM) facility in Lowell, Massachusetts, and the Textron Systems facility in Wilmington, Massachusetts. The thermal cycling efforts at the Textron Systems used a Thermotron Model F-32-CHV-705 thermal chamber. The thermal cycling conducted at the Cobham (M/A-COM) facility used a Tenney Environmental Model T20C-1.5 thermal chamber. In addition, a Watlow F4 controller and Watview software was used to control the thermal chamber. Prior to thermal cycling, all assembled test vehicles received accelerated thermal aging consisting of a bake-out period of 24 hours at 100 $^{o}$C.

The parameters used for the thermal cycling included a maximum temperature of 125 $^{o}$C and a minimum temperature of -55 $^{o}$C, resulting in a total temperature differential of 180 $^{o}$C between the high and low temperature extremes. These maximum and minimum temperatures are based upon IPC-9701, Test condition #4. The low temperature dwell time was fifteen minutes, and the high temperature dwell time was fifteen minutes. The temperature ramp rate was approximately 5 $^{o}$C per minute.

Therefore, the overall cycle time was 102 minutes (36 minutes temperature ramp up + 15 minutes high temperature dwell + 36 minutes temperature ramp down + 15 minutes low temperature dwell). The thermal profile is illustrated in the figure below:

**Figure 1:**
**Thermal Cycling Temperature Profile**

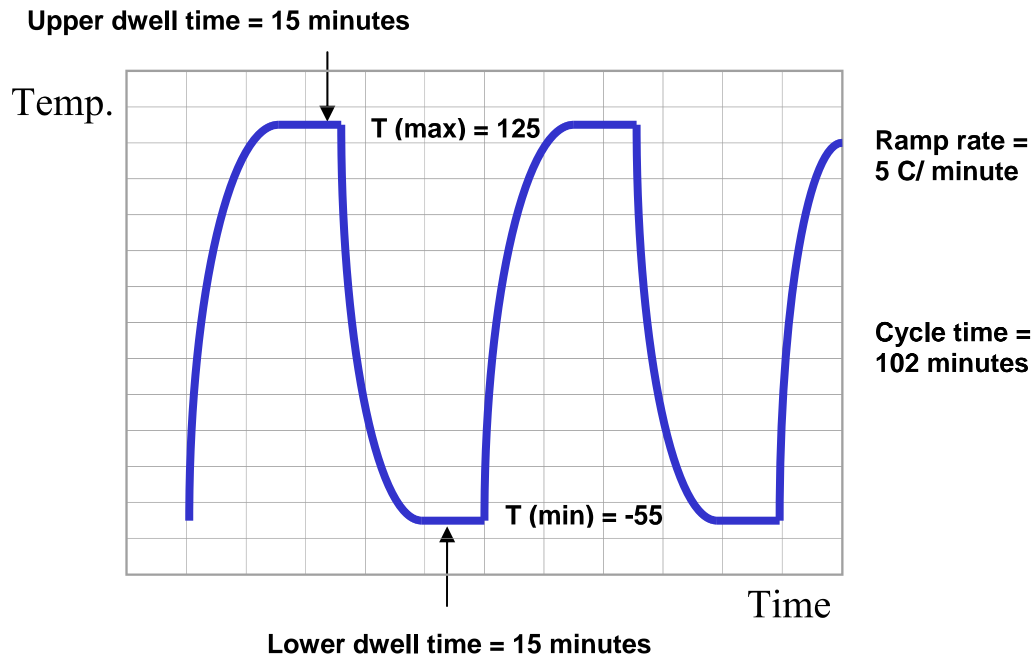


2.2 Vibration Testing
The vibration testing was conducted at the Raytheon facility located in Towson, Maryland. The test vehicles were vibrated until 63% failures were generated. Four test vehicles were mounted to the vibration fixture at one time. Twelve test vehicles were included in the vibration test, including 8 lead-free test vehicles and and 2 tin/lead test vehicles. The sixteen test vehicles included in the thermal cycling are listed in the table below.

**Table 3:**
**Test Vehicles Included in Thermal Cycling**

| Test Vehicle | SMT Solder Paste | Through Hole Solder | Surface Finish | PWB Laminate |
| --- | --- | --- | --- | --- |

| Test Vehicle | SMT Solder Paste | Through Hole Solder | Surface Finish | PWB Laminate |
|---|---|---|---|---|
| 1 | SAC 305 NC-1 | SAC305 | ENIG | High Tg FR4 |
| 3 | SAC 305 NC-1 | SAC305 | LF HASL | High Tg FR4 |
| 5 | SAC 305 NC-1 | SAC305 | OSP | High Tg FR4 |
| 7 | SAC 305 NC-1 | SAC305 | Nanofinish | High Tg FR4 |
| 9 | SAC 305 OA | Tin/copper (295 C) | ENIG | High Tg FR4 |
| 11 | SAC 305 OA | Tin/copper (295 C) | LF HASL | High Tg FR4 |
| 13 | SAC 305 OA | Tin/copper (295 C) | OSP | High Tg FR4 |
| 15 | SAC 305 OA | Tin/copper (295 C) | Nanofinish | High Tg FR4 |
| 17 | SAC 305 NC-2 | Tin/copper (310 C) | ENIG | High Tg FR4 |
| 19 | SAC 305 NC-2 | Tin/copper (310 C) | LF HASL | High Tg FR4 |
| 21 | SAC 305 NC-2 | Tin/copper (310 C) | OSP | High Tg FR4 |
| 23 | SAC 305 NC-2 | Tin/copper (310 C) | Nanofinish | High Tg FR4 |
| 25 | Tin/lead NC | Tin/Lead | ENIG | High Tg FR4 |
| 27 | Tin/lead NC | Tin/Lead | LF HASL | High Tg FR4 |
| 29 | Tin/lead NC | Tin/Lead | OSP | High Tg FR4 |
| 31 | Tin/lead NC | Tin/Lead | Nanofinish | High Tg FR4 |

Similar to the thermal cycling, the same components and daisy chain configuration was utilized for the vibration testing. Also the same failure definition and data logger was used for resistance monitoring for the vibration testing. The following were the target shock levels and duration used for the vibration testing:

X axis: no vibration
Y axis: no vibration
Z axis: see below for vibration spectrum.

1 hour at Level 1 (approximately 2 grms)
1 hour at Level 2 (approximately 4 grms)
1 hour at Level 3 (approximately 6 grms)
1 hour at Level 4 (approximately 8 grms)

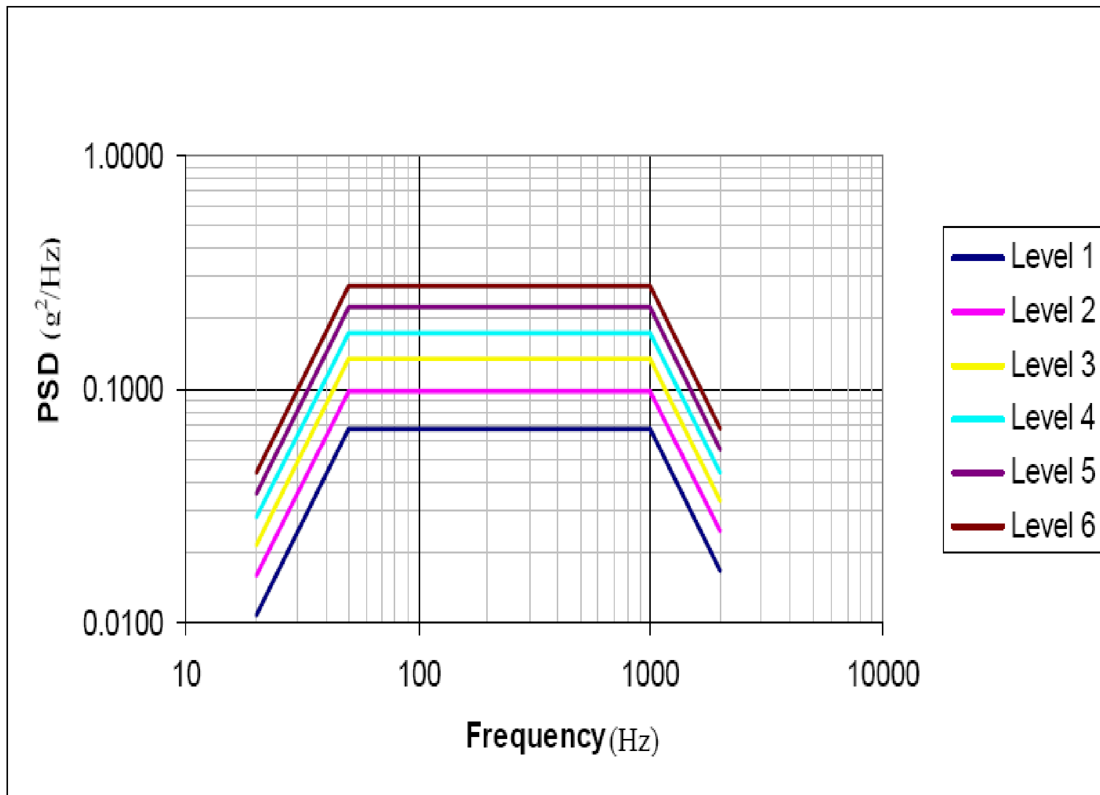


All assembled test vehicles received accelerated thermal aging consisting of a bake-out period of 24 hours at 100 degrees C prior to undergoing vibration testing.

The test fixture for the vibration testing was designed by Raytheon. The purpose of this fixture was to hold four test vehicles at the same time. This significantly reduced the overall time required to conduct the vibration testing. The test vehicles were mounted to the vibration fixture using screws at each of the four corners of the test vehicle. Due to the concern of potential intermittent connector failures during vibration testing, teach of the daisy chain wires from the data logger were soldered to the test vehicle In addition, structural epoxy was applied to these wires to provide strain relief. The following figure shows the vibration testing setup.

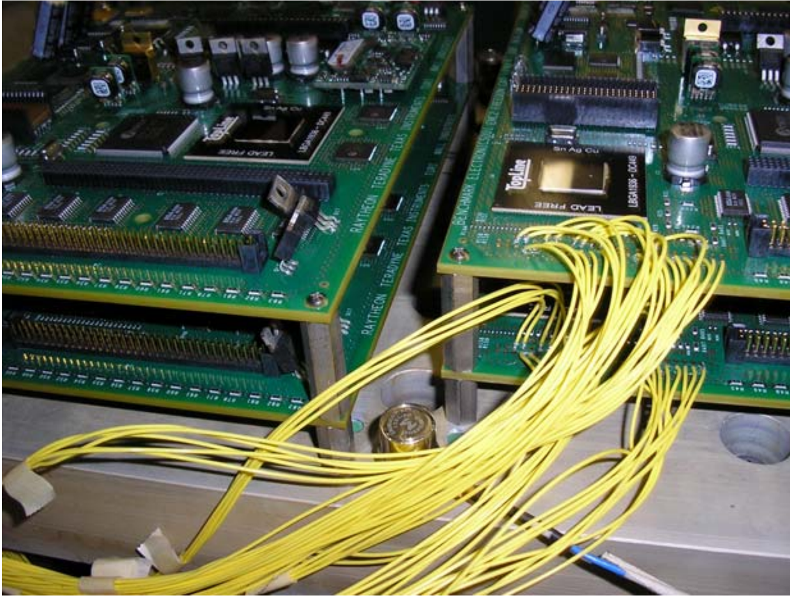

Figure X: Solder connections to the test vehicle for data logger wires.

An accelerometer was mounted in the center of each test vehicle. This allowed the vibration levels to be measured at the center of the test vehicle where the vibration would be the greatest because it was the furthest distance from the fixture mounting locations at the four corners of the fixture. The following tables provides the vibration levels measured at the center of the test vehicle for each of the different vibration input levels.

| **Input Vibration** | **Vibration Measured at the Center of the Test Vehicle** |
|---|---|
| 2 grms | Approx. 11 grms |
| 4 grms | Approx. 20 grms |

| 6 grms | Approx. 29 grms |
| --- | --- |
| 8 grms | Approx. 37 grms |

Table X: Vibration Levels at the Center of the Test Vehicle

# 3.0 Results and Discussion

## 3.1 Thermal Cycling

| Event | Thermal Cycle |
| --- | --- |
| Start thermal cycling at Textron Systems | 0 |
| Concurrent component failures on 2 halogen-free boards not in DOE | 220 |
| Stop thermal cycling at Textron Systems, and start thermal cycling at Cobham | 1,000 |
| As of 1,470 cycles, there had been 82 component failures recorded before the occurrence of any concurrent component failures | 1,470 |
| Concurrent component failures on 8 of 16 boards in DOE | 1,479 – 2,204 |
| Stop thermal cycling at Cobham | 2,204 |

Test Vehicle #12

| Channel | Board and REFDES | Component Type | Failure Cycle |
| --- | --- | --- | --- |
| 4029 | Bd 12: 0805-1 | Resistor 0805 | 801 |
| 4024 | Bd 12: 0805-2 | Resistor 0805 | 809 |
| 4015 | Bd 12: 0603 | Resistor 0603 | 929 |
| 4021 | Bd 12: U25 | TSOP 48 Pins | 972 |
| 4032 | Bd 12: 0402 | Resistor 0402 | 1,129 |

| 4031 | Bd 12: U26 | MicroBGA 84 | 1,490 |
|---|---|---|---|
| 4018 | Bd 12: U16 | CABGA 100 | 1,718 |
| 4033 | Bd 12: U17 | MicroBGA 64 | 1,718 |
| 4035 | Bd 12: U14 | PBGA 256 | 1,718 |
| 4023 | Bd 12: U18 | PBGA 256 | 1,718 |
| 4026 | Bd 12: U15 | PQFP 208 | 1,718 |
| 4013 | Bd 12: U1 | TSOP 48 Pins | 1,718 |
| 4027 | Bd 12: U2 | TSOP 48 Pins | 1,718 |
| 4022 | Bd 12: U24 | TSOP 48 Pins | 1,718 |

Continuity testing conducted to investigate the concurrent failures.

Conducted on 18 test vehicles after they went through 2,204 thermal cycles

Conducted on 4 TSOPs (U1, U2, U24, and U25) and two BGAs (U17 and U26) per test vehicle

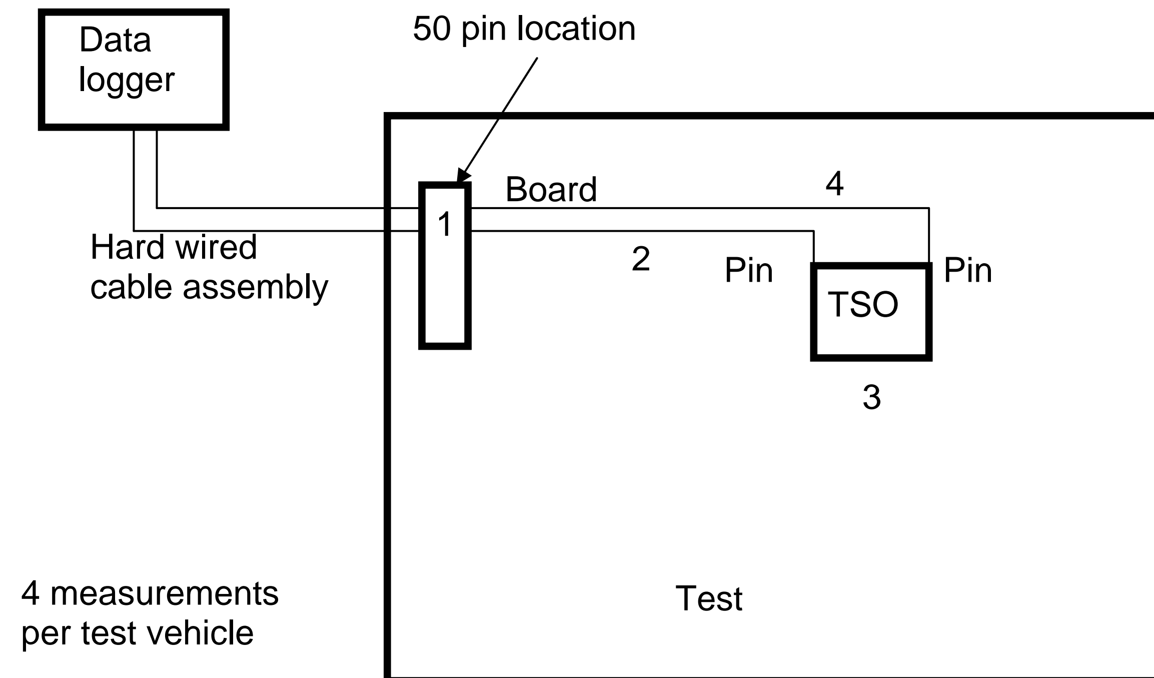


Board trace measurements

**Instance:**
If there is a greater than 100% increase in measured resistance in the trace from the component to the J2 location after thermal cycling

**Test vehicles with concurrent component failures:**
11 instances out of 43 components tested

**Test vehicles without concurrent component failures:**
0 instances out of 36 components tested

Test vehicles with concurrent failures appear to have test vehicle/trace failures. This would result in confounding between component and test vehicle failures during thermal cycles 1,479 to 2,204. Consequently, the thermal cycling analysis was done with data up to 1,470 thermal cycles.

Halogen free laminates, At 220 cycles, $P = 0.00$
There is a statistically significant difference between standard FR4 and halogen-free laminate material for failures of total SMT components during thermal cycling.

For the purposes of analyzing the results of the thermal cycling data, a minimum of 63% of failures is required in order to plot the Weibull distribution. Therefore, the Weibull distribution was only provided for the component types that achieved a minimum of 63% failures during thermal cycling. Once the Weibull plot was generated for a component type, then various points of interest can be calculated such as the number of cycles to 1% cumulative failure ($N_1$), number of cycles to 50% cumulative failure ($N_{50}$), or characteristic life ($N_{63}$)

The two test vehicles with halogen-free laminate material had early failures for all components. The components on the two test vehicles with halogen-free laminate material had all failed by 220 thermal cycles.

The thermal cycling data was recorded, collected, and analyzed for 1,470 thermal cycles. A summary of the thermal cycling failure data for the sixteen test vehicles in the DOE is provided in the table below for the daisy chains connected to only one component.

**Table 4:**
**Thermal Cycling Data for Daisy Chains with One Component**

| Component RefDes | Component Type | Number of Failures | Number of Daisy Chains | Percent Failed |
|---|---|---|---|---|
| U16 | Chip array BGA, 100 balls (1.0 mm pitch) | 12 | 16 | 75.0% |
| U17 | Tape array microBGA, 64 balls (0.5 mm pitch) | 9 | 16 | 56.3% |

| Comp-onent RefDes | Component Type | Number of Failures | Number of Daisy Chains | Percent Failed |
|---|---|---|---|---|
| U26 | Ceramic microBGA, 84 balls (0.5 mm pitch) | 8 | 16 | 50.0% |
| U1, U2, U24, U25 | TSOP, 48 Pins | 13 | 56 | 23.2% |
| U15 | PQFP, 208 pins | 1 | 16 | 6.3% |
| U14, U18 | Plastic BGA, 256 balls (1.0 mm pitch) | 1 | 32 | 3.1% |

The component located at reference designator U16 was the only component to surpass the 63% threshold prior to the onset of interconnect failures at 1,470 thermal cycles.

The other components included in the thermal cycling are the surface mount resistors. Each of these components only has two solder joint terminations per component, whereas the components in the table above have between 48 to 256 solder joint connections per component. A summary of the thermal cycling failure data after 1,470 thermal cycles is provided in the table below for the daisy chains connected to more than one component.

**Table 5:**
**Thermal Cycling Data for Daisy Chains with More Than One Component**

| Component Type | Quantity of Components per Daisy Chain | Number of First Failures | Number of Daisy Chains | Percent of Daisy Chains with First Failure |
|---|---|---|---|---|
| 0805 Resistor | 49 - 52 | 23 | 32 | 71.9% |
| 0402 Resistor | 100 | 8 | 16 | 50.0% |
| 0603 Resistor | 100 | 7 | 16 | 43.8% |

The three different resistors (0805, 0603, and 0402) are industry standard packages. The primary difference between the resistors is physical size. The 0805 resistor is the largest, and the 0402 resistor is the smallest. The 0402 resistor had the highest percentage (71.0%) of daisy chains where the first failure was identified.

The U16 component is a surface mount component that is a chip array ball grid array. The component has 100 balls, a 1.0 millimeter pitch, and an 11 millimeter body size. The ball matrix size is 10 millimeters by 10 millimeters. For components assembled on the tin/lead test vehicles, the solder ball material is eutectic tin lead solder. For the components assembled on the lead-free test vehicles, the solder ball material is SAC solder. The package thickness is 1.5 millimeters, and the package material is bismaleimide-triazine. (Practical, 2007) The coefficient of thermal expansion for the U16 component and the two laminate materials are provided in the table below (Isola, 2006).

**Table 6:**
**Coefficient of Thermal Expansion for U16 and Laminate Materials**

| Material | Coefficient of Thermal Expansion (ppm/$^{o}$C) |
|---|---|
| Component: chip array ball grid array bismaleimide-triazine | 18 |
| Laminate: High Tg FR4 (X and Y axis) | Pre Tg, 13<br>Post Tg, 14 |
| Laminate: Halogen-free (X and Y axis) | Pre Tg, 13<br>Post Tg, 14 |

There is a coefficient of thermal expansion delta of 5 ppm/ $^{o}$C below the glass transition temperature ($T_g$), and a coefficient of thermal expansion delta of 4 ppm/ $^{o}$C below the glass transition temperature ($T_g$).

Weibull probability plots were used to model the failure data obtained during the thermal cycling testing. The two parameter Weibull distribution is defined by the following two parameters: shape and scale. The shape parameter describes the shape of the Weibull curve. A shape value of "3" approximates a normal curve. A shape value between "2" and "4" is still somewhat normal. A shape value lower than two low describes a right-skewed curve, and a shape value greater than four describes a left-skewed curve. The scale parameter is the 63.2 percentile ($N_{63.2}$) of the data. The scale parameter is sometimes referred to as characteristic life. The scale value defines the position of the Weibull curve relative to the threshold. For example, a scale value of 10, indicates that 63.2% of the equipment will fail in the first 10 units (hours, cycles, etc.) following the threshold time. The Weibull probability density function used by Minitab is as follows. (Minitab, 2008)

$$F(x) = \{ax^{a-1} * e^{-(x/b)a}\} / ba, x>0 \quad (10)$$

Eight out of the twelve lead-free test vehicles have experienced failures for the U16 component. The shape parameter calculated for U16 on lead-free test vehicles is 0.54, and the scale parameter calculated for U16 on lead-free test vehicles is 932.7. The following figure shows the Weibull distribution for the U16 component on lead-free test vehicles.

**Figure 2:**
**Weibull Distribution for the U16 Component on Lead-free Test Vehicles**

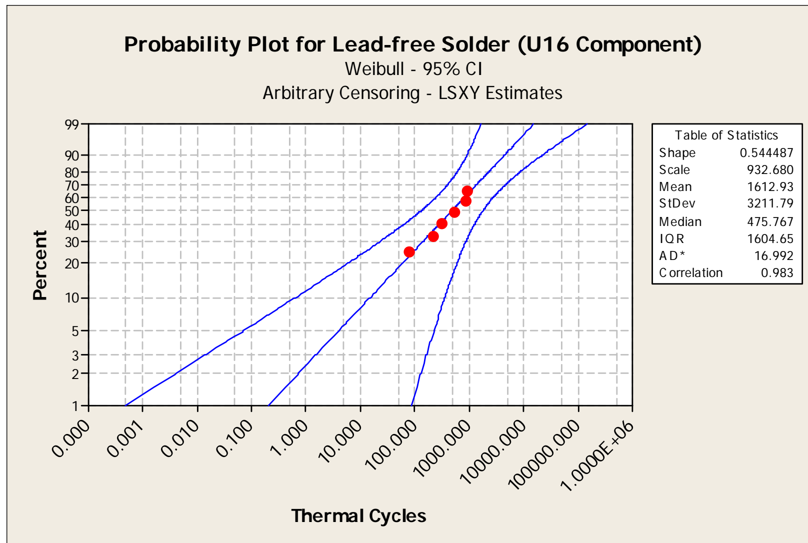


All of the four tin/lead test vehicles have experienced failures for the U16 component. The shape parameter calculated for U16 on tin/lead test vehicles is 1.06, and the scale parameter calculated for U16 on tin/lead test vehicles is 718.3. The following figure shows the Weibull distribution for the U16 component on tin/lead test vehicles.

**Figure 3:**
**Weibull Distribution for the U16 Component on Tin/Lead Test Vehicles**

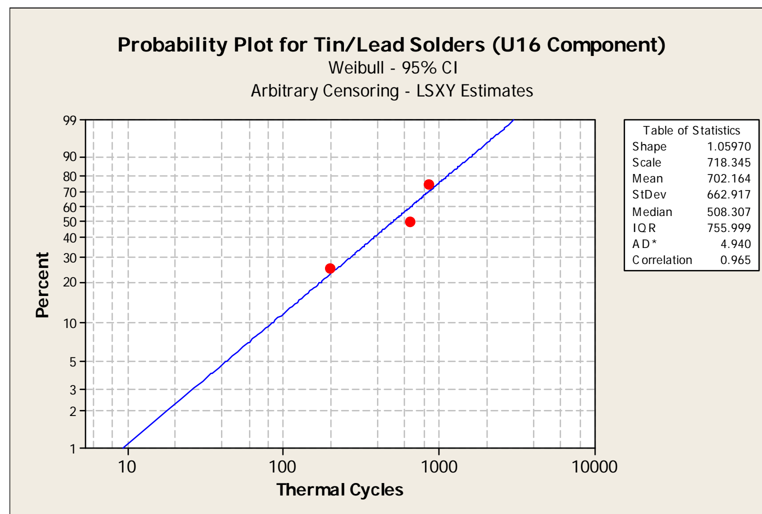


The Weibull distribution is used to determine the percent of test vehicles that are anticipated to fail by a particular time under test conditions. In this case, it is the percent of test vehicles that are anticipated to fail by a certain number of thermal cycles under test conditions. The Table of Percentiles provided by Minitab for both the lead-free and tin/lead test vehicles for the U16 component is provided in the table below.

**Table 7:**
**Table of Percentiles for U16 Component**

| Percent | Designation | Lead-free Percentile | Tin/lead Percentile |
|---|---|---|---|

| Percent | Designation | Lead-free Percentile | Tin/lead Percentile |
|---|---|---|---|
| 1 | $N_1$ | 0.2 | 9.4 |
| 10 | $N_{10}$ | 15.0 | 85.9 |
| 20 | $N_{20}$ | 59.3 | 174.4 |
| 30 | $N_{30}$ | 140.4 | 271.5 |
| 40 | $N_{40}$ | 271.6 | 381.1 |
| 50 | $N_{50}$ | 475.8 | 508.3 |
| 60 | $N_{60}$ | 794.3 | 661.5 |
| 63.2 | $N_{63.2}$ (scale value) | 932.7 | 718.3 |
| 70 | $N_{70}$ | 1,311.6 | 855.9 |
| 80 | $N_{80}$ | 2,235.2 | 1,125.6 |
| 90 | $N_{90}$ | 4,314.9 | 1,578.1 |

This information can be interpreted as ten percent ($N_{10}$) of the U16 components on tin/lead test vehicles will fail during thermal cycling conditions after approximately 86 thermal cycles, and seventy percent ($N_{70}$) of the U16 components on lead-free test vehicles will fail during thermal cycling conditions after approximately 1,311 thermal cycles. For the component U16, the tin/lead test vehicles appear more robust from $N_1$ through $N_{50}$. However, there is a crossover point after $N_{50}$, and from $N_{60}$ through $N_{90}$ the lead-free test vehicles appear more robust. This indicates that there may be two different failure modes involved, one is possibly an infant mortality related failure mode and the other is possibly a wear out mechanism failure mode. (O'Connor, 2002) This is further evidence for this situation because there are four lead-free test vehicles that have not had failures for the U16 component, however, there have been U16 failures to date for all four of the tin/lead test vehicles.

**Failure analysis**

**Scope:**

Five 48 pin TSOPs (Boards: 12, 14, 16, 6, 28 and chips: U1, U1, U24, U2, U1 respectively.

Six microBGAs with 64 balls (U17 on Boards: 18, 32, 2, 6, 3, and 11).

**Thermal Imaging:**

Power was applied to the components because a defect would cause an increase in the resistance. This resistance increase would in turn increase the energy in that particular location when electricity is induced. The thermal imaging camera was used to locate temperature differences in the components when they were powered.

**Cross Sectioning:**

Once the location of the defect on the component is determined, cross sectioning is done to examine the damage.

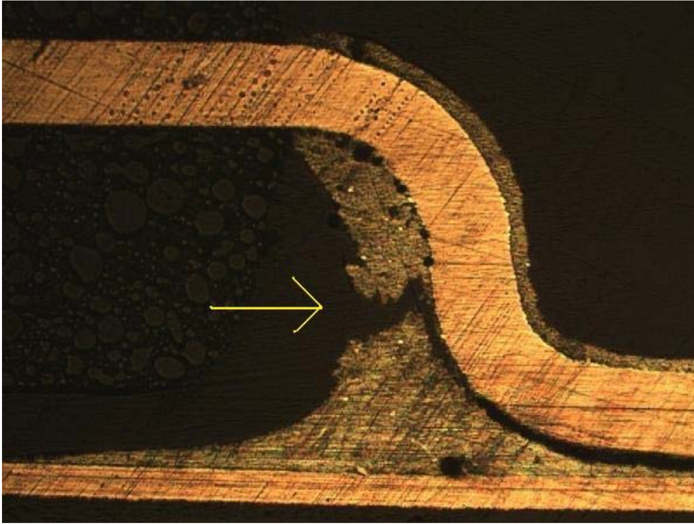

Solder joint crack initiated at the heel fillet and propagated to the toe fillet

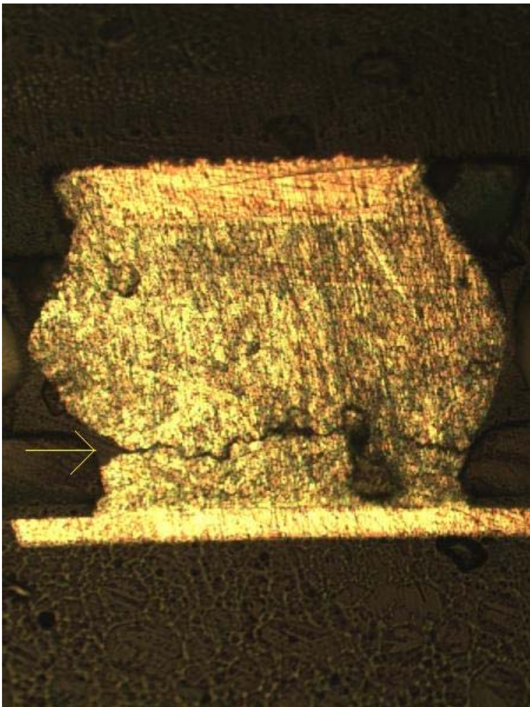

# Crack in microBGA solder joint

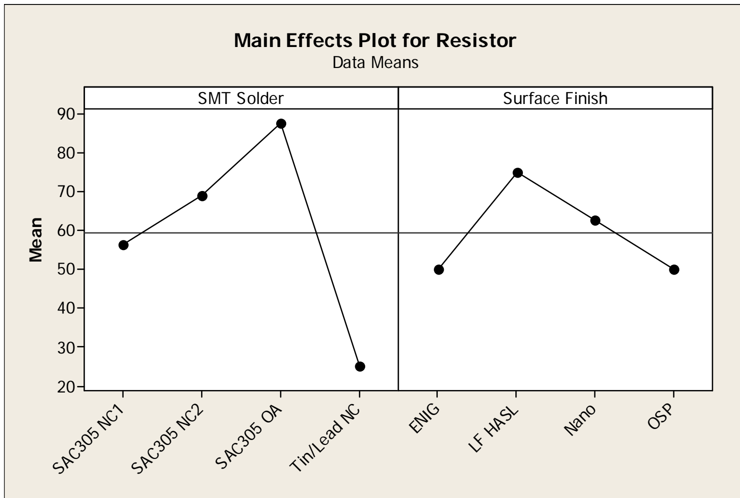


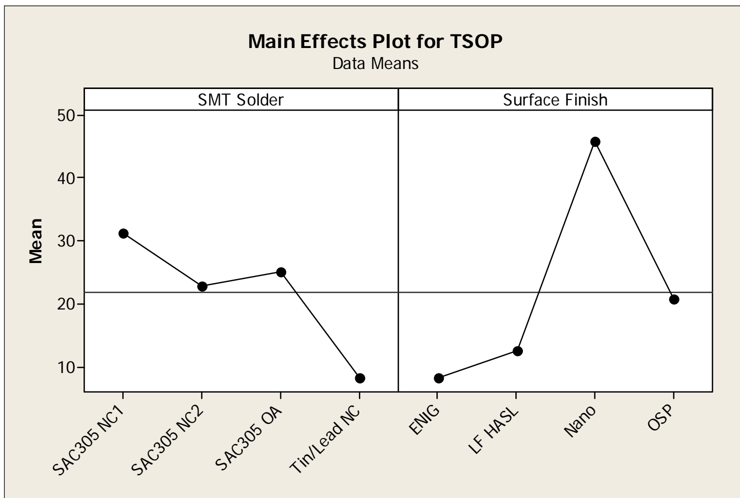

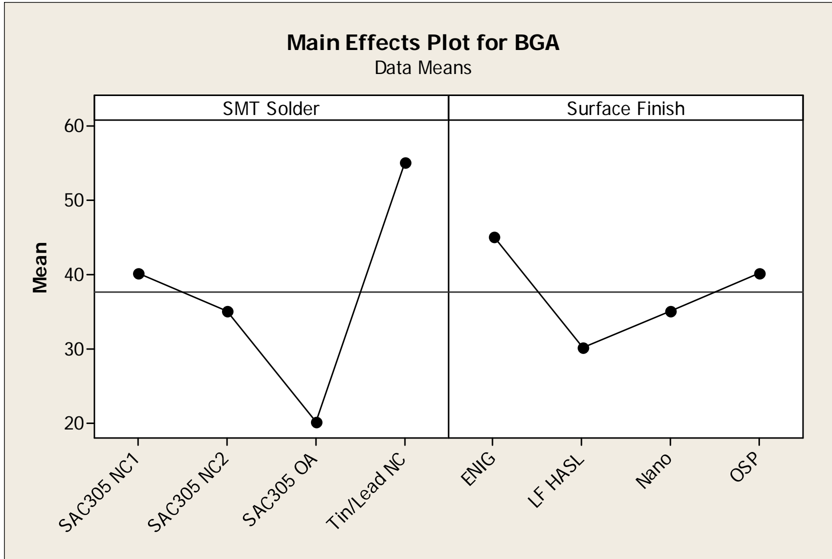


## 3.2 Vibration Testing

The following table provides a summary of the vibration test results.

| Event | Time |
|---|---|
| Start vibration testing at 2 grms | 0 hours |
| Complete vibration testing at 2 grms with no component failures. Start vibration testing at 4 grms. | 1 hour |
| Complete vibration testing at 4 grms with no component failures. Start vibration testing at 6 grms. | 2 hours |
| There had been 5 component failures recorded before the occurrence of any concurrent component failures | 2 hours 51 minutes |
| Concurrent component failures occur on all 12 test vehicles. After 3 hours the vibration level is increased to 8 grms. | 2 hours 52 minutes to 3 hours 52 minutes |
| Stop vibration testing | 4 hours |

| Vibration | Duration | Lead-free Test Vehicles (Qty. 8) | Tin/lead Test Vehicles (Qty. 4) |
|---|---|---|---|
| 2 grms | 1 hour | No failures | No failures |
| 4 grms | 1 hour | No failures | No failures |

| | | | |
|---|---|---|---|
| 6 grms | 1 hour | 3056 (TSOP, U1) at 38 minutes<br>3001 (TSOP, U25) at 41 minutes<br>2056 (TSOP, U25) at 43 minutes<br>2001 (TSOP, U25) at 45 minutes | 4021 (TSOP, U25) at 48 minutes<br>TV #27, #31 at 52 minutes<br>4048 (TSOP, U1) at 55 minutes |
| 8grms | 1 hour | TV #19, #23 at 10 minutes<br>TV #7, #9 at 11 minutes<br>3057 (TSOP, U24) at 14 minutes<br>3048 (TSOP, U1) at 20 minutes<br>TV #1, #17 at 22 minutes<br>3066 (BGA, U26) at 24 minutes<br>TV #5, #15 at 52 minutes | 4036 (TSOP, U25)at 1 minute<br>4050 (Res. 0603) at 3 minutes<br>4067 (Res. 0402) at 7 minutes<br>TV #25, #29 at 22 minutes |

| Channel | Test Vehicle and REFDES | Component Type | Time to Failure (minutes) |
|---|---|---|---|
| 3047 | Bd 15: U16 | CABGA 100 | 161 |
| 3046 | Bd 15: U26 | MicroBGA 84 | 184 |
| 3051 | Bd 15: 0402 | Resistor 0402 | 232 |
| 3045 | Bd 15: 0603 | Resistor 0603 | 232 |
| 3039 | Bd 15: 0805-1 | Resistor 0805 | 232 |
| 3044 | Bd 15: 0805-2 | Resistor 0805 | 232 |
| 3041 | Bd 15: U15 | PQFP 208 | 232 |
| 3052 | Bd 15: U17 | MicroBGA 64 | 232 |
| 3043 | Bd 15: U18 | PBGA 256 | 232 |
| 3037 | Bd 15: U2 | TSOP 48 Pins | 232 |
| 3042 | Bd 15: U24 | TSOP 48 Pins | 232 |
| 3036 | Bd 15: U25 | TSOP 48 Pins | 232 |
| 3069 | Bd 15: U14 | PBGA 256 | 233 |

Failure distribution 4 TSOPs and 2 BGAs

| Component Failure Type | Quantity | Percentage of Total |
|---|---|---|
| | | |

| Failure: concurrent | 56 | 85% |
|---|---|---|
| Failure: non-concurrent (5 before first concurrent failure occurred) | 10 | 15% |
| No failure | 0 | 0% |
| Total | 66 | 100% |

**Continuity testing**
**Instance:**
If there is a greater than 100% increase in measured resistance in the trace from the component to the J2 location after thermal cycling

**For 12 Test Vehicles after vibration testing:**
2 instances found out of 54 components tested (TSOPs and BGAs)

- Based on the results of the continuity testing, the test vehicles with concurrent failures appear to have test vehicle/interconnect failures.
- Not enough data for statistical analysis of component failures that occurred before onset of test vehicle/interconnect failures

## 4.0 Conclusions

The test conditions within the thermal cycling chamber are much more severe than most operating environments for electronics products. The intent was to accelerate aging and produce early failures. The two test vehicles with halogen-free laminate material had early failures for all components. The components on the two test vehicles with halogen-free laminate material had all failed by 220 thermal cycles. Therefore, there appears to be major reliability issues with the halogen free laminate based upon the thermal cycling test conditions used in this research. However, the test vehicles assembled using the halogen-free laminate material experienced early failures during the thermal cycling and therefore this is considered to be a potentially significant reliability issue.

The sixteen test vehicles included in the Design of Experiments that had the high Tg FR4 laminate material have proven to be robust. Only one component (U16 BGA) out of the nine different component types being monitored for failures had exceeded the 63% failure threshold after experiencing 1,470 thermal cycles. Based upon the Weibull plot results for the U16 component, the tin/lead test vehicles appear more robust from the percentiles $N_1$ through $N_{50}$. However, there is a crossover point after $N_{50}$, and from $N_{60}$ through $N_{90}$ the lead-free test vehicles appear more robust. This indicates that there may be two different failure modes involved, one is possibly an infant mortality related failure mode and the other is possibly a wear out mechanism failure mode.

## 6.0 Acknowledgements

The authors would like to acknowledge the contributions from the following individuals and corporations for their support of this research:

John Goulet, JoAnn Newell, Robert Farrell, Paul Bodmer, Bruce Tostevin, Allen Ouellette, and Scott Mazur, Benchmark Electronics, Hudson, NH. Mike Havener, Benchmark Electronics, Winona Minnesota. David Pinsky, Amit Sarkhel, and Karen Ebner, Raytheon. Rob Tyrell, Stentech, Don Lockard, Yankee Soldering. Eric Ren and Deb Fragoza, EMC. Andy Lesko and Bernhard Wessling, Ormecon. Don Longworth, Tom Buck, and Wendi Boger Dynamic Details Inc. Linda Darveau, U.S. EPA Region 1. Helena Pasquito and Dick Anderson, Cobham (M/A-COM). George Wilkish, Prime Consulting. Roger Benson, Carsem. Scott Miller, Wendy Milam, and Lauren Primmer, Freedom CAD. Crystal Wang, International Rectifier. Don Abbot, Texas Instruments. Ken Degan, Teradyne. Steven Sekanina, Isola. Mike Jansen, Mike Miller and Louis Feinstein Textron Systems. Charlie Bickford, Wall Industries. Paul Reid and Bill Birch, PWB Interconnect Solutions. Tim O'Neill and Karl Seelig, Aim Solder. Lou Wroblewski, Premier Tool Works.

## 7.0 Literature Cited

Brist, Gary, Long, Gary, Lead-free Product Transition: Impact on Printed Circuit Board Design and Material Selection, APEX Designers Summit, February 2005.

Crowe Dana, Feinberg, Alec, Design for Reliability, CRC Press, Boca Raton, pp. 9-1 through 9-16, 2001.

Engelmaier, Werner, Solder Joint Reliability – Part 3: Comparing Different Solder Fatigue Models, Global SMT & Packaging, pp. 35 – 36, August, 2002.

Engelmaier, Werner, How to Establish Models for Reliability, Overcoming the Reliability Challenge, IPC Summit, April 16, pp. 1 – 27, 2008.

IPC–TM-650, Test Methods Manual, DC Current Induced Thermal Cycling Test, May 2001.

IPC-9701 Standard “Performance Test Methods and Qualification Requirements for Surface Mount Solder Attachments”, IPC Association Connecting Electronics Industries, pp. 1-3 through 1-6, January 2002.

Isola, Isola IS 500 Product Data Sheet, pp. 1 – 2, May 8, 2006.

Isola, Isola 370HR Product Data Sheet, pp. 1 – 2, August 29, 2006.

Lee, W.W., et. al., Solder Joint Fatigue Models: Review and Applicability to Chip Scale Packages, Microelectronics Reliability, 40, pp. 231 – 244, 2000

Manock, John, et al., Effect of Temperature Cycling Parameters on the Solder Joint Reliability of a Pb-free PBGA Package, SMTA Journal, Volume 21 Issue 3, pp. 36 – 45, 2008.

Mei, Zequn, TSOP Solder Joint Reliability, IEEE, 0-7803-3286, pp. 1232 – 1238, May, 1996.

Minitab, Interpreting the Shape, Scale, and Threshold on a Weibull Probability Plot, www.minitab.com/support/answers, August 2008.

Norris, K. C., Landzberg, A. H., Reliability of Controlled Collapse Interconnections, IBM Journal of Research and Development, pp. 266-271, May 1969.

O’Connor, Patrick D. T., Practical Reliability Engineering, Fourth Edition, John Wiley & Sons Ltd, West Sussex, England, pp. 4 – 20, 2002.

Pan, N., An Acceleration Model for Sn-Ag-Cu Solder Joint reliability Under Various Thermal Cycle Conditions, SMTAI, pp. 876-883, 2006.

Practical Components, Product Catalogue - Chip Array Ball Grid Array, pp. 12 – 14, 2007.

PWB Interconnect Solutions, Inc., IST Test E08_0089_Preliminary Results-As Received Testing-XS, pp. 1 – 56, July 28, 2008.

PWB Interconnect Solutions, Inc., Understanding IST Technology, http://www.pwbcorp.com/FrameDoc.html, August, 2008.

Shina, Sammy G., Green Electronics Design and Manufacturing – Reliability of Green Electronic Systems, McGraw-Hill, New York, pp. 67 – 129, 2008.

Syed, Ahmer, Doty, Matthew, Are We Over Designing for Solder Joint Reliability? Field vs. Accelerated Conditions, Realistic vs. Specified Requirements, Electronic Components and Technology Conference, IEEE, pp. 111 – 117, 1999.

United States Patent 7342317, Low Coefficient of Thermal Expansion Build-up Layer Packaging and Method Thereof, http://www.patentstorm.us/patents/7342317/fulltext.html March 11, 2008.

Yasukawa, Akio, A New Index S for Evaluating Solder Joint Thermal Fatigue Strength, IEEE Transactions on Components, Hybrids, and Manufacturing technology, Vol. 13, No. 4, pp. 1146 – 1153, December, 1990.